

Dat H. Nguyen^{1,2,3,*}

Michael E. Colvin^{4,5}

Yin Yeh⁶

Robert E. Feeney⁷

William H. Fink¹

¹Department of Chemistry,
University of California,
Davis, CA 95616

²Department of Computer
Science,
University of California,
Davis, CA 95616

³Division of Computational
and Systems Biology,
Lawrence Livermore National
Laboratory,
Livermore, CA 94550

⁴Schools of Natural Sciences
and Engineering,
University of California,
Merced, CA 95344

Intermolecular Interaction Studies of Winter Flounder Antifreeze Protein Reveal the Existence of Thermally Accessible Binding State

⁵Division of Physical
Biosciences Institute,
Lawrence Livermore National
Laboratory,
Livermore, CA 94550

⁶Department of Applied Science,
University of California,
Davis, CA 95616

⁷Department of Food Science
and Technology,
University of California,
Davis, CA 95616

Received 14 January 2004;

accepted 19 April 2004

Published online 01 July 2004 in Wiley InterScience (www.interscience.wiley.com).

DOI 10.1002/bip.20104

Abstract: *The physical nature underlying intermolecular interactions between two rod-like winter flounder antifreeze protein (AFP) molecules and their implication for the mechanism of antifreeze function are examined in this work using molecular dynamics simulations, augmented with free energy calculations employing a continuum solvation model. The energetics for different modes of interactions of two AFP molecules is examined in both vacuum and aqueous phases along with the*

Correspondence to: Dr. Dat H. Nguyen; email: dnguyen@hms.harvard.edu; or Dr. William H. Fink; email: fink@chem.ucdavis.edu.

*Present address: Department of Genetics, Harvard Medical School, Boston, MA 02115.

Biopolymers, Vol. 75, 109–117 (2004)

© 2004 Wiley Periodicals, Inc.

water distribution in the region encapsulated by two antiparallel AFP backbones. The results show that in a vacuum two AFP molecules intrinsically attract each other in the antiparallel fashion, where their complementary charge side chains face each other directly. In the aqueous environment, this attraction is counteracted by both screening and entropic effects. Therefore, two nearly energetically degenerate states, an aggregated state and a dissociated state, result as a new aspect of intermolecular interaction in the paradigm for the mechanism of action of AFP. The relevance of these findings to the mechanism of function of freezing inhibition in the context of our work on Antarctic cod antifreeze glycoprotein (Nguyen et al., *Biophysical Journal*, 2002, Vol. 82, pp. 2892–2905) is discussed. © 2004 Wiley Periodicals, Inc. *Biopolymers* 75: 109–117, 2004

Keywords: biological antifreeze; winter flounder; protein dimer; protein–protein interactions; molecular dynamics (MD)

INTRODUCTION

The survival of many polar fishes during the winter is dependent on their bodies' ability to inhibit and suppress the growth of ice crystals when the temperature of the seawater and therefore the fish's blood serum falls well below freezing.^{1,2} It has been determined that the unusually low freezing temperature of fish blood serum cannot be attributed to colligative effects of dissolved substances (such as salts) alone, but is due to the presence of a family of so-called biological antifreezes.^{3–6} Biological antifreezes can be classified into two categories according to the presence or absence of carbohydrate moieties. The former are known as antifreeze glycoproteins, while the latter are known as antifreeze proteins.^{5,7–25} Biological antifreezes are known macroscopically not only to prevent the growth of the incipient ice crystals up to several degrees below freezing, but also to interfere with the growth morphology of ice crystals and, in a noncolligative manner, to exhibit thermal hysteresis, which lowers the freezing temperature without affecting the melting temperature. Furthermore, thermal hysteresis is additive to the colligative effect. Early hypotheses of the mechanism of function were based on data from the ice etching technique developed by Knight et al.^{26–28} Although particular facets for antifreeze protein (AFP) and antifreeze glycoprotein (AFGP) accumulation can be identified, this method lacks the ability to characterize adsorption dynamics. Hence, initial postulates suggested that the proteins are irreversibly adsorbed onto the surface of particular facets. It was the work of Kuroda²⁹ in 1991 that questioned the irreversible binding aspect of the hypothesis.

Winter flounder AFPs are type I AFPs and consist mostly of two components, namely HPLC6 and HPLC8, of which the former (which we will subsequently refer to as AFP) is the major component and the subject of this study. This AFP's chemical composition consists of 37 amino acid residues and has been a subject of intensive experimental and compu-

tational studies. Both the X-ray crystallography³⁰ and the NMR^{31,32} structures of AFP have now been determined and show that it is a rod-like α -helix protein (Figure 1). It has been long believed that AFP functions directly on the exposed ice surface along the (20 $\bar{1}$) crystal plane by means of a hydrogen-bonding network. The interaction is postulated to be between the regularly spaced Thr residues and the matching water molecule that is capable of hydrogen bonding with Thr for the particular facet in question. As a result of the direct interaction, hysteresis, due to the Kelvin effect (see ref. 1 for more details), is observed. However, works since 1997 using site-directed mutagenesis of winter flounder AFP^{33–36} showed that hydrogen bonding between this molecule and the ice may not be responsible for thermal hysteresis. Harding et al.³⁷ suggested that it is the hydrophobic interactions including entropic contributions at the facet-specific ice–water interface that contribute to the ability of antifreeze proteins to accumulate selectively due to favorable total free energy of the system. Thus, the exact molecular mechanism of action of biological antifreezes at the molecular level awaits elucidation.

While there have been a number of simulation studies examining the interactions of a single AFP in solution and ice surface–AFP interactions,^{38–43} the physical underlying nature of intermolecular interactions of two AFP has not been examined by a simulation study. In this article, we present a simulation study examining the intermolecular interactions of two AFP molecules, starting in a vacuum and then in solution.

MODEL OF AFP–AFP INTERACTIONS

The mechanism of action of AFP has long been proposed to be one of competitive inhibition, whereby the protein competes favorably for the growth sites of the ice crystal. When the competition favors the protein, crystal growth is inhibited; when the reverse becomes true, faceted ice growth commences.

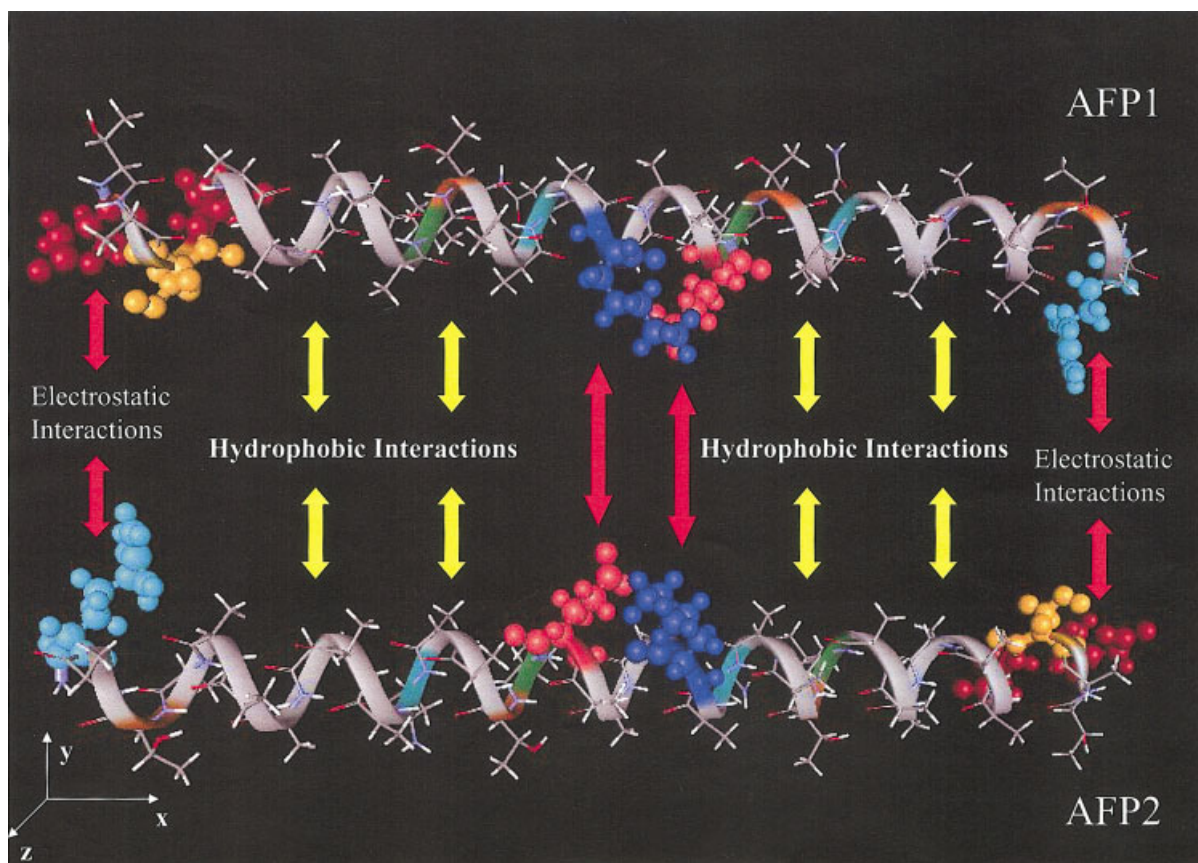


FIGURE 1 Two winter flounder antifreeze protein molecules in the anti-parallel configuration.

Here we will focus on another approach. We look for the total free energy constraints when two AFP molecules are placed in an anti-parallel fashion. AFP has an intriguing structural feature, as one may observe, in that the two peptides' sequences on opposite molecules would perfectly complement each other in terms of electrostatic as well as hydrophobic interactions. This structural observation is pictorially shown in Figure 1. This hypothetical interaction geometry would allow maximum complementarity of both electrostatic interactions between charged side chains of aspartic acid 1 and 5, lysine 18, glutamic acid 22, and arginine 37 residues of one AFP to the same amino acid residues but in the opposite order and hydrophobic interactions between two relatively nonpolar backbones. From the protein-protein interaction perspective, the electrostatic and nonpolar complementarities are crucial driving forces for the binding mode and stability of enzyme/ligand complexes and have been the subject of many studies during the past decade on the nature of mechanism of enzyme/substrate binding.^{44,45} As a result, we propose that, upon this structural observation, these intermolecular interactions

between two anti-parallel AFP molecules may well have an important role in retarding the growth of the ice crystal. Therefore, in this work, we examine three specific aspects of intermolecular interactions between two AFP molecules. First, we examine intrinsic interactions of two anti-parallel AFP molecules as a function of distance between two anti-parallel helical axes and a function of the rotational angle about each helical axis in a vacuum. We restrict our attention to planar arrangements of the helical axis. We realize that this restriction may preclude finding the definitive minimum geometry complex, but believe that we will sample those geometries where the coulomb interactions of the side chains will be maximized, since any angle between the helical axes necessarily moves these side chains further apart. Second, we examine the free energy of association of two AFP molecules for several geometrically parallel modes of interactions in water. Finally, we examine hydrophobicity, in terms of free energy of water distribution, in the region bounded by two anti-parallel AFP backbones as a function of distance between two helical axes.

METHODS

The X-ray structure of the AFP molecule³⁰ (code 1WFB) was used as a starting structure for our simulations. Since there are two HPLC6 AFP molecules in the unit cell, the one with the straightest α -helical axis structure was taken and the other was discarded. Because our study explores the interaction between two AFP, we chose the straighter structure so that the interacting geometries would be better defined. The resulting structure will be referred to as AFP1 (Figure 1). The AFP1 molecule was rotated in such a way that its principal axes aligned along three principal cartesian x -, y -, and z -axes as defined in Figure 1. A copy of AFP1, referred to as AFP2, was then rotated 180° about its x -axis and 180° about the y -axis in order to obtain an anti-parallel structure (Figure 1) with respect to AFP1. To aid the discussion that follows, all distances discussed in this article are defined as the distance between two parallel or anti-parallel helical axes, and all rotational angles are referred to as the rotational angle about the α -helical axis (x -axis) with respect to the original face-to-face orientation shown in Figure 1. The dynamics was performed using the AMBER 5.0 program package⁴⁶ with a Cornell '94 all-atom force field.⁴⁷

AFP–AFP Interactions in a Vacuum

The nature of AFP–AFP intrinsic interactions is probed by computing the total energy of the AFP1–AFP2 systems in a vacuum for different geometrically parallel modes of interactions. We studied the dependence of these interactions on two coordinates; first, the total potential energy of the AFP1–AFP2 system is computed as a function of distance; and second, the total potential energy is computed as a function of rotational angle (around the axes of the AFPs). In the first case, the AFPs were simulated with interaxis distances of 13, 14, 15, 16, 17, 18, 19, 25, 30, 35, and 40 Å, resulting in 11 systems. A molecular dynamics (MD) simulation was carried out for each of these systems for 0.5 ns at a constant temperature of 300 K after an equilibration process, which consisted of 5000 iterations of minimization using conjugate gradient and 110 ps of equilibration. In all MD simulations, backbone atoms (N, C $_{\alpha}$, and C) were held fixed in space while all remaining atoms were allowed to move freely; no potential truncation was applied, and snapshots of the trajectory were saved periodically every 0.5 ps. Similarly, in the second case, both AFP1 and AFP2 were placed at a separation distance of 15.0 Å, a distance giving a minimum energy as determined from the first case, and each AFP1 and AFP2 was rotated in turn with an increment of 90° about its helical axis, resulting in 16 AFP1–AFP2 systems. While a complete search would require examining this rotational orientation at all distances to verify that the most attractive complex had been found, here we simply confirm that the orientation with the charged groups facing each other is more energetically favorable. Our search grid in either distance or angle is not sufficiently fine to locate the most attractive conformation in a vacuum; rather it is

designed simply to search for the possible existence of a general preference in mutual orientation of two monomers. Besides, since the focus of this work is on the free energy of attraction between two AFP molecules in solution, such a complete search in a vacuum would not be necessary. The simulation protocol used in the second case is exactly as in the first case.

Free Energy of Association

The free energy of association of two AFP molecules for different modes of interaction was computed as follows: two AFP molecules were placed at a distance of 10 Å, which is the closest interhelical distance without atomic overlapping, in parallel and anti-parallel fashion with two orientations such that their charged sides face away from each other (180° rotational angle) and directly toward each other (0° rotational angle). We examined these four systems designated configurations A, B, C, and D. In configurations A and B, both AFP molecules are anti-parallel to each other, but in the former configuration, charges face away from each other, and in the latter configuration, charges face directly toward each other (as shown in Figure 1). Configurations C and D are defined similarly, but the AFP molecules are parallel to each other. Each of these four systems was solvated in a box of ~ 3800 TIP3P water molecules⁴⁸ and MD was carried out for 0.5 ns using the NPT ensemble with the temperature held fixed at 300 K using Berendsen's algorithm⁴⁹ and pressure maintained at 1.0 atm using isotropic scaling, after 10,000 iterations of minimization (using conjugate gradient) and 0.3 ns of equilibration. Particle-mesh Ewald⁵⁰ was used for handling long-range forces while the potential function was truncated at 10.0 Å for short-range forces (van der Waals forces). In the PME, the grid size of ~ 1.0 Å was used in conjunction with the error tolerance of 10^{-5} . Snapshots from the trajectory were saved periodically every 2.0 ps. The time step was set to 2.0 fs in conjunction with the SHAKE algorithm⁵¹ for restraining all bonds containing hydrogen atoms, with the SHAKE geometrical error tolerance set to 10^{-4} Å. In addition, a simulation of a single AFP in aqueous water, whose simulation protocol is exactly as described above, was carried out to allow computation of free energy of association. The free energy of association was computed from the saved trajectory using the MM-PBSA method as previously reported.⁵² Details of parameters used in the MM-PBSA method are reported in our previous work.⁵³

Hydrophobic Nature in the Region Encapsulated by AFP1–AFP2

As the last objective of this study, we examined the hydrophobic nature, in terms of free energy of water distribution, in the region encapsulated by two helical backbones of AFP1–AFP2. As in the vacuum simulations, we anchored both AFP1 and AFP2 in an antiparallel orientation with their charged sides facing each other (i.e., in Figure 1) in such a way that the distances between AFP1 and AFP2 were

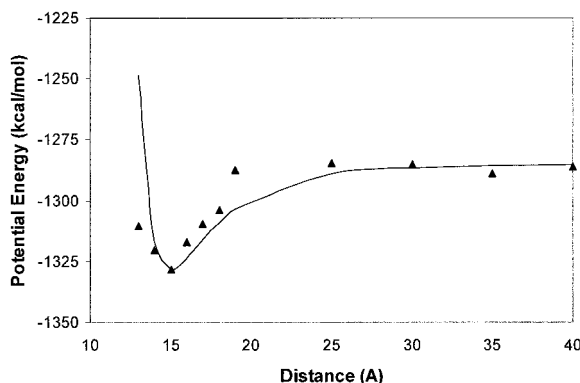


FIGURE 2 Potential energy profile of the AFP1–AFP2 as a function of inter-AFP distance. Calculated results are shown as triangles. The standard error associated with each potential average is ~ 0.4 kcal/mol. The solid line helps visualize the results presented so that the attractive potential of ~ 40 kcal/mol and the distance at which minimum occurs is readily seen.

at 13, 15, 18, 21, 24, 27, 30, and 33 Å, resulting in eight systems. Each of these AFP1–AFP2 systems was then immersed into a box of 4555 TIP3P water molecules. The minimization was carried out for 10,000 iterations using the conjugate gradient method, followed by the 50 ps of constant pressure and 100 ps of constant volume MD. Each simulation was completed with another 200 ps of MD using the NVT ensembles with the temperature held fixed at 300 K. During the course of dynamics, all backbone atoms were fixed to ensure the well-defined region bounded by two AFPs. The trajectory was saved periodically every 0.25 ps.

To improve the statistics, we performed another three sets of simulations using thermal perturbation of different heating schemes. In the first set, all atom velocities saved at the end of the equilibration above were reassigned a new velocity drawn randomly from the Maxwellian distribution at 200 K; then thermally ramped to 330 K within a 10 -ps period; run at this temperature for another 10 ps; cooled down to 300 K within another 10 ps; and finally equilibrated for another 100 ps. Each solvated system of the first set was simulated further for 200 ps of MD. A similar procedure was applied for the remaining two sets, but the initial temperatures were 230 and 260 K, respectively, and the ramped temperatures were at 360 and 390 K, respectively. These four sets of MD simulations allowed us to obtain better statistics for the water distribution in the region bounded by AFP1–AFP2.

RESULTS AND DISCUSSION

In this section, we present three sets of results corresponding to three sets of simulations described in the previous section along our discussion of their rele-

vance to the mechanism of function of biological antifreezes.

AFP–AFP Intrinsic Interactions in a Vacuum

The energy of interactions in a vacuum can provide a means for studying the intrinsic intermolecular interactions of AFP molecules in the absence of all other external influences such as solvation. We therefore chose this regime to measure the interaction strength of AFP1 and AFP2 as a function of distance and of rotational angle. Figure 2 presents the total potential energy profile of the AFP1–AFP2 as a function of distance, while Figure 3 shows the corresponding profile as a function of the rotational angle along each AFP's helical axis whose interhelical distance is at 15.0 Å. In Figure 2, triangles represent the average total energies of AFP1–AFP2 systems over the period of dynamics, visually aided by the solid line plotted from the Lennard–Jones potential function ($U_{LJ}=4*\epsilon [(\sigma/r)^{12}-(\sigma/r)^6]$) with $\epsilon \sim 40$ kcal/mol and σ approximately 13 Å. In Figure 3, the angle θ_1 is defined as the rotational angle of the AFP1 molecule about its α -helical axis, whereas θ_2 is the corresponding one of AFP2. A value of zero of these two variables corresponds to the configuration where both charged faces of AFP1 and AFP2 face each other (as shown in Figure 1), while other values correspond to the degrees for which each angle is rotated about its helical

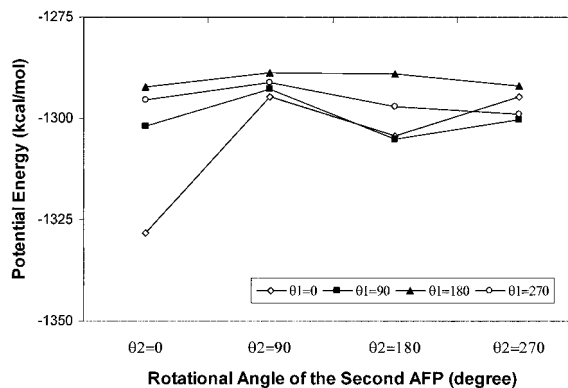


FIGURE 3 Potential energy profile of the AFP1–AFP2 as a function of orientational interaction between AFP1 and AFP2 at interhelical axes distance of 15 Å. Unfilled diamonds start with the original face-to-face orientation of the dimer as AFP2 is rotated about its helical axis, while AFP1 held fixed ($\theta_1 = 0$). Similarly, filled squares, unfilled circles, and filled triangles represent configurations where AFP1 is rotated by 90, 180, and 270°, respectively. The standard error associated with each potential average is ~ 0.4 kcal/mol.

Table I Free Energy of Interactions of Two AFP Molecules for Different Configurations

		E_{MM}		E_{PB}		E_{NP}		E_{subtotal}		$E_{\text{entropy}} (-TS)$		
Configurations		Ave.	St. Err.	Ave.	St. Err.	Ave.	St. Err.	Ave.	St. Err.	Ave.	St. Err.	Total
Individual conformational free energy	A	-685.1	2.2	-644.9	1.7	31.7	0.0	-1298.2	1.2	-698.5	2.9	-1996.7
	B	-746.3	2.2	-598.4	1.5	30.6	0.0	-1314.1	1.5	-708.2	5.0	-2022.3
	C	-719.1	2.0	-631.6	1.6	32.5	0.1	-1318.2	1.3	-698.2	3.6	-2016.4
	D	-665.7	1.7	-675.3	1.0	31.3	0.0	-1309.7	1.4	-701.1	2.8	-2010.8
	Single AFP	-334.0	1.3	-326.3	0.8	19.8	0.0	-640.5	0.9	-371.6	2.9	-1012.1
Free energy of association	A	-17.0		7.7		-7.8		-17.1		44.6		27.5
	B	-78.3		54.2		-9.0		-33.1		35.0		1.9
	C	-51.1		21.0		-7.1		-37.2		44.9		7.7
	D	2.4		-22.7		-8.3		-28.6		42.0		13.4

axis. The standard errors—defined as the ratio of the standard deviation over the square root of the number of snapshots—for data points in Figures 2 and 3 are about 0.4 kcal/mol. As can be seen clearly from Figures 2 and 3, the AFP1–AFP2 configuration, where charged sides face each other in an anti-parallel fashion, is the most favorable with a magnitude of interaction strength of about 40 kcal/mol spatially at the interhelical distance of 15.0 Å and about 25 kcal/mol rotationally. Given the magnitude of statistical standard error mentioned above computed for the vacuum case, the anti-parallel mode of interactions between AFP1 and AFP2 is indeed the most favorable. It confirms our intuitive expectation on the intrinsic mode of AFP intermolecular interactions.

Free Energy of Association of AFP1–AFP2

The free energies of association between two AFP molecules can provide insight into the energetics of their intermolecular behaviors in solution and, in the end, the effect of solvation on their intrinsic intermolecular interactions can be extracted. Therefore, in this part of the paper, we examine the free energies of association of two AFP molecules in a combination of parallel or anti-parallel configurations and with their charged sides facing each other or away from each other. These four configurations we label configurations A–D. As mentioned before, configurations A and B are similar in that they are anti-parallel, while configurations C and D are parallel. The charged sides of both AFP molecules face away from each other in configurations A and C, while they face toward each other in configurations B and D. The free energies of association for all four configurations are shown in

Table I. As shown, all free energies of association of these four AFP1–AFP2 systems are positive, which is consistent with experimental observation that AFP exists in solution as a monomer. However, it is clear that the free energy of association of configuration B (our proposed configuration illustrated in Figure 1) is the most favorable one with free energy of ~ 1.9 kcal/mol. Given the magnitude of the standard error of about a few kcal/mol (see Table I), the free energy of configuration B can be considered a thermally accessible associative state. Further detailed analysis of individual contribution of each energy component to the MM-PBSA free energy expression (also in Table I) shows that the intrinsic intermolecular attractive behavior between two AFP molecules is still preserved, as the force-field energy term E_{MM} shows. However, this E_{MM} term is almost completely counterbalanced by solvation and entropy effects upon association. These imply that while AFP1 and AFP2 are intrinsically attractive to each other, water and entropy will prevent them from aggregating. However, the existence of the thermally accessible associative state may be important in the mechanism of ice inhibition as discussed below.

Hydrophobicity in the Inter-AFP Region

The term “hydrophobicity” carries a variety of meanings in the literature. An aspect that we have chosen to use as a marker for hydrophobic influences is free energy of water distribution around the solute. We compute this free energy of water distribution in this region using the potential of mean force method by binning the average of the water distribution along the α -helical axis over the course of dynamics, followed by the normalization to the highest water containing

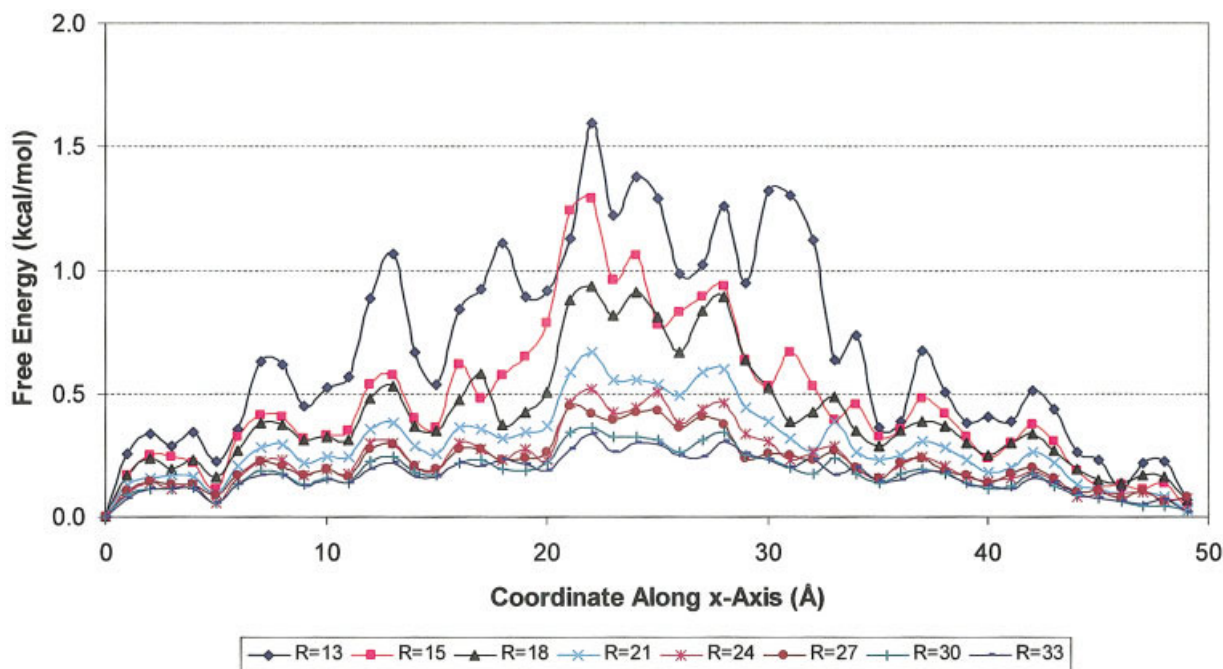


FIGURE 4 Free energy of water distribution in the region between two helical axes along the x -axis. Each curve from the top to the bottom represents the water distribution of each simulated configuration where the inter-AFP distances increase from 13.0 to 33 Å, respectively.

bin, and then converting the relative populations to an energy with the aid of the Boltzmann distribution. A bin size of 1.0 Å was used. In the hydrophobic regions of a particular solute, the free energy of water distribution would be expected to be higher than a corresponding one in the less hydrophobic (more hydrophilic) region. We computed this measure of hydrophobicity in the region bounded by two anti-parallel AFP molecules and Figure 4 depicts the free energy of water distribution in this region. As can be seen, the free energy of water distribution is lower toward the two ends of the AFP molecules than in the middle of the region, indicating that the space between the two molecules is indeed hydrophobic by our definition.

Relevance of Simulation Results to Biological Antifreeze Function

In the discussion above, we present data indicating the intrinsic behaviors and the existence of the thermally accessible associative state of two AFP molecules. The relevance of AFP-I interactions in a broader perspective of the mechanism of function of the diverse structures of all the AFPs identified to date must also be raised, since there are not similar structural motifs to exploit for the other AFPs. Looking beyond the immediacy of structure of AFP-I to the results of the simulations, the threads that might generalize are

the creation of a mass and energy flux barrier, the former by means of accumulation in the interfacial region; and the latter by the availability of multiple states that can act as an energy reservoir and that interfere with dissipation of the local energy fluctuation caused by those water molecules that set onto the ice lattice. From our simulation results of the possible existence of a thermally accessible state for the association of two AFP molecules in solution, one can hypothesize that the AFP-I would function as a thermal reservoir that, in effect, could retard the growth rate of the ice crystal locally where it accumulates on the ice surface. This conjecture on the mechanism of action of AFP-I is also consistent with the observed properties of the antifreeze process, such as the hysteresis governed by the rule known as the Kelvin (or Gibbs–Thompson) relation. The main distinction between this and earlier hypotheses on the function of antifreeze proteins is that it changes the emphasis in the mechanism from one based exclusively on the binding to ice to one that includes the concept of local energy transfer (or energy coupling). We do not see this change in emphasis at variance with the view that AFP-I functions as a monomer when it adsorbs on the ice surface.⁵⁴ In this revised view, the ice growth rate of areas on the ice surface, where AFP-I accumulates, is lower than the ice growth rate of areas on the ice surface, where there is no accumulation of AFP-I, and

therefore, manifests Kelvin effects. This hypothesized mechanism is similar to that from our previous work on the Antarctic cod⁵³ (*Pathogenia borchgrevink*) antifreeze glycoprotein (AFGP-8), where we found that AFGP-8 has multiple degenerate states in its conformational energy landscape. As a result, AFP-I can act as a thermal reservoir in a similar fashion as AFGP-8. From these considerations, we begin to see a possible common mechanism for both of these proteins, even though they are completely different both chemically and structurally.

CONCLUSIONS

We have examined molecular interactions of two AFP molecules, exploring rotational degrees of freedom about the helical axes and the distance between the helical axes in both vacuum and aqueous environments with MD and probed the hydrophobic nature in the region bounded by two anti-parallel AFP molecules. We observed the intrinsic characteristic nature of interactions of two anti-parallel AFP molecules under various conditions and this intrinsic mode of interaction is counterbalanced by solvation and entropy, therefore preventing them from aggregating in solution, which is consistent with experimental observation. However, the presence of a thermally accessible state involving the association of two AFP molecules in an anti-parallel fashion is intriguing and may contribute to the antifreeze mechanism, as we previously proposed.⁵³ Clearly, however, any role of this state remains highly speculative. Its role, if any, may be established either by MD simulations presenting the ice-water interface to AFP molecules or by experimental observations implying the involvement of such a state. Nonetheless, even if this state, which resulted from the intermolecular interaction of AFP molecules, plays no role in the antifreeze mechanism, the question remains as to why this protein would have evolved a structure able to form a perfectly paired anti-parallel configuration. A central lesson of biology is that there are usually reasons for nature's designs; we expect that further studies of this anti-parallel interaction motif in AFP-I in the presence of water/ice interface will help illuminate further the detailed mechanism of function of this interesting protein.

D.H.N acknowledges Lawrence Livermore National Laboratory predoctoral fellowship (SEGRF) support. This work was in part carried out at Lawrence Livermore National Laboratory under Contract W-7405-ENG-48 from the U.S. Department of Energy.

REFERENCES

1. Yeh, Y.; Feeney, R. E. *Chem Rev* 1996, 96, 601–618.
2. Fletcher, G.; Hew, C.; Davies, P. *Annu Rev Physiol* 2001, 63, 359–390.
3. Scholander, P.; Dam, L.; Kanwisher, J.; Hammel, T.; Gordon, M. *J Cell Comp Physiol* 1957, 49, 5–24.
4. DeVries, A. L.; Wohlschlag, D. E. *Science* 1969, 163, 1073–1075.
5. DeVries, A. L.; Komatsu, S. K.; Feeney, R. E. *J Biol Chem* 1970, 245, 2901–2908.
6. Scholander, P. F.; Maggert, J. E. *Cryobiology* 1971, 8, 371–374.
7. DeVries, A. L. *Science* 1971, 172, 1152–1155.
8. DeVries, A. L.; Vandenheede, J.; Feeney, R. E. *J Biol Chem* 1971, 246, 305–308.
9. DeVries, A. In *Animals and Environmental Fitness*; Gilles, R., Ed.; Pergamon Press: Oxford, 1980, pp. 583–607.
10. DeVries, A. L. *Annu Rev Physiol* 1983, 45, 245–260.
11. Komatsu, S.; DeVries, A. L.; Feeney, R. E. *J Biol Chem* 1970, 245, 2909–2913.
12. Duman, J. G. ; DeVries, A. L. *Cryobiology* 1972, 9, 469–472.
13. Feeney, R.; Hofmann, R. *Nature* 1973, 243, 357–359.
14. Feeney, R. E. *Am Sci* 1974, 62, 712–719.
15. DeVries, A. In *Fish Physiology*; Hoar, W.; Randall, D., Eds.; Academic Press: London, 1971, pp. 157–190.
16. Hew, C. L.; Joshi, S.; Wang, N. C.; Kao, M. H.; Ananthanarayanan, V. S. *Eur J Biochem* 1985, 151, 167–172.
17. Duman, J. G. ; DeVries, A. L. *Nature* 1974, 247, 237–238.
18. Duman, J. G. ; DeVries, A. L. *Comp Biochem Physiol B* 1976, 54, 375–380.
19. Ng, N. F.; Hew, C. L. *J Biol Chem* 1992, 267, 16069–16075.
20. Ng, N. F.; Trinh, K. Y.; Hew, C. L. *J Biol Chem* 1986, 261, 15690–15695.
21. Slaughter, D.; Fletcher, G. L.; Ananthanarayanan, V. S.; Hew, C. L. *J Biol Chem* 1981, 256, 2022–2026.
22. DeLuca, C. I.; Chao, H.; Sonnichsen, F. D.; Sykes, B. D.; Davies, P. L. *Biophys J* 1996, 71, 2346–2355.
23. Jia, Z.; DeLuca, C. I.; Davies, P. L. *Protein Sci* 1995, 4, 1236–1238.
24. Sonnichsen, F. D.; DeLuca, C. I.; Davies, P. L.; Sykes, B. D. *Structure* 1996, 4, 1325–1337.
25. Deng, G. J.; Andrews, D. W.; Laursen, R. A. *FEBS Lett* 1997, 402, 17–20.
26. Knight, C. A. ; DeVries, A. L. *Science* 1989, 245, 505–507.
27. Knight, C. A. ; DeVries, A. L. *J Crystal Growth* 1994, 143, 301–310.
28. Knight, C. A.; Cheng, C. C. ; DeVries, A. L. *Biophys J* 1991, 59, 409–418.
29. Kuroda, T. *Proceedings of the 4th Topical Conference on Crystal Growth Mechanisms, Japan, 1991*, pp. 157.
30. Sicheri, F.; Yang, D. S. *Nature* 1995, 375, 427–431.

31. Gronwald, W.; Chao, H.; Reddy, D. V.; Davies, P. L.; Sykes, B. D.; Sonnichsen, F. D. *Biochemistry* 1996, 35, 16698–16704.
32. Sonnichsen, F. D.; Davies, P. L.; Sykes, B. D. *Biochem Cell Biol* 1998, 76, 284–293.
33. Chao, H.; Houston, M. E., Jr.; Hodges, R. S.; Kay, C. M.; Sykes, B. D.; Loewen, M. C.; Davies, P. L.; Sonnichsen, F. D. *Biochemistry* 1997, 36, 14652–14660.
34. Haymet, A. D.; Ward, L. G.; Harding, M. M.; Knight, C. A. *FEBS Lett* 1998, 430, 301–306.
35. Haymet, A.; Ward, L.; Harding, M. *J Am Chem Soc* 1999, 121, 941–948.
36. Haymet, A. D.; Ward, L. G.; Harding, M. M. *FEBS Lett* 2001, 491, 285–288.
37. Harding, M. M.; Ward, L. G.; Haymet, A. D. *Eur J Biochem* 1999, 264, 653–665.
38. Sansom, C. E.; Atkins, E. D. T.; Upstill, C. In *Gums and Stabilisers for the Food Industry*; Phillips, G.; Wedlock, D.; Williams, P., Eds.; Elsevier: London, 1986.
39. Lal, M.; Clark, A.; Lips, A.; Ruddock, J.; White, D. *Faraday Discuss* 1993, 95, 299–306.
40. Chou, K. C. *J Mol Biol* 1992, 223, 509–517.
41. Jorgensen, H.; Mori, M.; Matsui, H.; Kanaoka, M.; Yanagi, H.; Yabusaki, Y.; Kikuzono, Y. *Protein Eng* 1993, 6, 19–27.
42. McDonald, S. M.; Brady, J. W.; Clancy, P. *Biopolymers* 1993, 33, 1481–1503.
43. Cheng, A.; Merz, K. M., Jr. *Biophys J* 1997, 73, 2851–2873.
44. Elcock, A.; Sept, D.; McCammon, J. *J Phys Chem B* 2001, 105, 1504–1518.
45. Jones, S.; Thornton, J. M. *Prog Biophys Mol Biol* 1995, 63, 31–65.
46. Case, D.; Pearlman, D.; Caldwell, J.; III, T. E. C.; Ross, W.; Simmerling, C.; Darden, T.; Merz, K.; Stanton, R.; Cheng, A.; Vincent, J.; Crowley, M.; Ferguson, D.; Radmer, R.; Seibel, G.; Singh, U.; Weiner, P.; Kollman, P. *AMBER 5*; University of California: San Francisco, 1997.
47. Cornell, W. D.; Cieplak, P.; Bayly, C. I.; Gould, I. R.; Jr., K. M. M.; Ferguson, D. M.; Spellmeyer, D. C.; Fox, T.; Caldwell, J. W.; Kollman, P. A. *J Am Chem Soc* 1995, 117, 5179–5197.
48. Jorgensen, W. L.; Chandrasekhar, J.; Madura, J. D.; Impey, R. W.; Klein, M. L. *J Chem Phys* 1983, 79, 926–935.
49. Berendsen, H. J. C.; Postma, J. P. M.; Gunsteren, W. F. v.; DiNola, A.; Haak, J. R.; *J Chem Phys* 1984, 3684–3690; *J Chem Phys* 1984, 81, 3684–3690.
50. Essmann, U.; Perera, L.; Berkowitz, M. L.; Darden, T.; Hsing, L.; Pedersen, L. G. *J Chem Phys* 1995, 103, 8577–8593.
51. Ryckaert, J. P.; Ciccotti, G.; Berendsen, H. J. C. *J Comput Phys* 1977, 23.
52. Srinivasan, J.; Cheatham, T. E.; Cieplak, P.; Kollman, P. A.; Case, D. A. *J Am Chem Soc* 1998, 120, 9401–9409.
53. Nguyen, D. H.; Colvin, M. E.; Yeh, Y.; Feeney, R. E.; Fink, W. H. *Biophys J* 2002, 82, 2892–2905.
54. Grandum, S.; Yabe, A.; Nakagomi, K.; Tanaka, M.; Takemura, F.; Kobayashi, Y.; Frivik, P. -E. *J Crystal Growth* 1999, 205, 382–390.

Reviewing Editor: Dr. C. Allen Bush